Lasers in Surgery and Medicine 36:193–201 (2005)

Chitosan Adhesive for Laser Tissue Repair: In Vitro Characterization

Antonio Lauto,[3]* J. Hook,[1] M. Doran,[1] F. Camacho,[1] L.A. Poole-Warren,[1] A. Avolio,[1] and L.J.R. Foster[2]
[1]*Graduate School of Biomedical Engineering, The University of New South Wales, 2052 New South Wales, Sydney, Australia*
[2]*School of Biotechnology and Bimolecular Sciences, The University of New South Wales, 2052 New South Wales, Sydney, Australia*
[3]*School of Chemistry, The University of New South Wales, 2052 New South Wales, Sydney, Australia*

Background and Objectives: Laser tissue repair usually relies on hemoderivate protein solders, based on serum albumin. These solders have intrinsic limitations that impair their widespread use, such as limited tensile strength of repaired tissue, poor solder solubility, and brittleness prior to laser denaturation. Furthermore, the required activation temperature of albumin solders (between 65 and 70°C) can induce significant thermal damage to tissue. In this study, we report on the design of a new polysaccharide adhesive for tissue repair that overcomes some of the shortcomings of traditional solders.
Study Design/Materials and Methods: Flexible and insoluble strips of chitosan adhesive (elastic modulus ~6.8 Mpa, surface area ~34 mm^2, thickness ~20 μm) were bonded onto rectangular sections of sheep intestine using a diode laser (continuous mode, 120 ± 10 mW, $\lambda = 808$ nm) through a multimode optical fiber with an irradiance of ~15 W/cm^2. The adhesive was based on chitosan and also included indocyanin green dye (IG). The temperature between tissue and adhesive was measured using a small thermocouple (diameter ~0.25 mm) during laser irradiation. The repaired tissue was tested for tensile strength by a calibrated tensiometer. Murine fibroblasts were cultured in extracted media from chitosan adhesive to assess cytotoxicity via cell growth inhibition in a 48 hours period.
Results: Chitosan adhesive successfully repaired intestine tissue, achieving a tensile strength of 14.7 ± 4.7 kPa (mean ± SD, $n = 30$) at a temperature of 60–65°C. Media extracted from chitosan adhesive showed negligible toxicity to fibroblast cells under the culture conditions examined here.
Conclusion: A novel chitosan-based adhesive has been developed, which is insoluble, flexible, and adheres firmly to tissue upon infrared laser activation. Lasers Surg. Med. 36:193–201, 2005. © 2005 Wiley-Liss, Inc.

Key words: biomaterials; solders; tissue welding

INTRODUCTION

Laser-activated solders for tissue repair are traditionally based on three proteins: albumin, fibrinogen, and collagen [1–5]. The first two are blood-derived and therefore have an intrinsic, although limited, risk of viral infection for the host organism [6,7]. Albumin solders are the most investigated and promising candidates for specific procedures in urology, vascular surgery and microsurgery due to their bonding characteristics [8–10]. Nevertheless, the use of albumin solders, especially in the solid form, is limited by their water solubility, lack of flexibility, and brittleness before being irradiated by lasers. These disadvantages, along with the potential thermal damage to tissue caused by the laser, may compromise the safe and reliable application of solders in surgical procedures [11,12]. It is not surprising therefore, that clinicians and surgeons are reluctant to routinely employ albumin solders for tissue repair and wound closure.

In a recent study, the addition of a natural crosslinking agent, genepin, to albumin based solders, resulted in enhanced bonding strength. Despite this, the unique albumin/genepin solder remained soluble and brittle [13]. Consequently, we have investigated alternative biopolymers in the design of a new tissue adhesive that overcomes shortcomings of currently used solders.

Chitosan is a polysaccharide derived from deacetylated chitin and can be readily solvent cast in a film that has excellent mechanical properties and low toxicity (Fig. 1) [14–17]. Chitosan may also bind to collagen as demonstrated by Taravel and Domard [18,19], who reported hydrogen bonding and polyanionic-polycationic interaction between these two biopolymers. In an attempt to improve bonding strength, Ono et al. [20] modified chitosan with lactobionic acid and *p*-azidebenzoic acid that was crosslinked with ultra-violet (UV) light on mice skin. The authors reported a maximum tensile strength of 3.1 kPa, significantly higher than the tensile strength of specimens bonded with fibrin (2.5 kPa). The same researchers showed that full-thickness skin wounds in mice healed after 8 days,

Contract grant sponsor: ARC discovery; Contract grant number: DPO345899; Contract grant sponsor: Engineering UNSW Faculty (2004).
*Correspondence to: Antonio Lauto, School of Chemistry, The University of New South Wales, 2052 NSW, Sydney, Australia. E-mail: antonio1@gsbme.unsw.edu.au
Accepted 13 December 2004
Published online 9 February 2005 in Wiley InterScience (www.interscience.wiley.com).
DOI 10.1002/lsm.20145

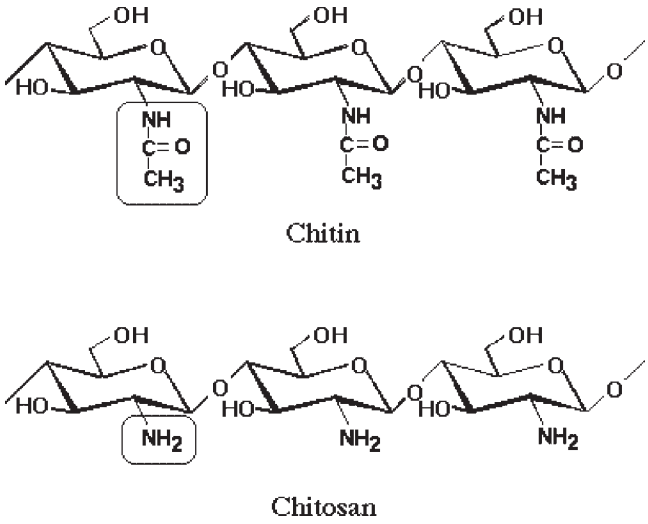

Fig. 1. Chemical structure of chitosan that is derived from deacetylated chitin.

if repaired with the modified chitosan gel and UV light. In contrast, untreated wounds healed slower, taking 11 days for closure. This chitosan gel was unfortunately water soluble prior to light crosslinking and therefore subject to fluid dilution like albumin solders.

In the present investigation, a chitosan-based film has been developed without UV-crosslinker modifications. The novel film is insoluble, flexible, and adheres firmly to tissue upon infrared laser activation.

MATERIALS AND METHODS

Chitosan Adhesive Film

Deacetylated chitosan ($\geq$85%) from crab shells (Sigma, St. Louis, MO) was dissolved to a concentration of $\sim$2% w/v in a water solution containing acetic acid ($\sim$2% v/v) and indocyanine green (IG, $\sim$0.02% w/v). The gelatinous chitosan solution (pH $\sim$4.0) was stirred for 6 hours before spreading evenly (thickness $\sim$2 mm, surface area $\sim$12 cm^2) over a clean, dry, perspex plate. The film was then dried for $\sim$6 days under clean conditions (atmospheric pressure, 25°C). The resulting chitosan films were carefully detached from the plate without damage and were insoluble in water and did not appear to swell. A digital caliper was used to measure the adhesive thickness, which ranged from 15 to 30 μm. Additional chitosan films without the dye IG were prepared using the same method.

All films were thereafter cut in rectangular strips ($\sim 7.5 \times 4.5$ mm), placed between glass slides to preserve their flat shape and stored in the dark at room temperature.

^{13}C-NMR

Solid-state ^{13}C-NMR spectra were acquired using a Varian Inova-300 spectrometer operating at 75.45 MHz with Chemagnetics 7.5 mm double air-bearing cross-polarization (CP) probe. Samples of chitosan shells and chitosan adhesive films ($\sim$200 mg) were packed as strips and pieces into 7.5 mm od rotors made from partially-stabilized zirconia and subjected to "magic-angle spinning" at 2–3 kHz. Spectra were acquired at 294 K using single-contact cross-polarization experiments with high-power ^{1}H decoupling during acquisition. The following parameters were found optimal: pulse width 5.2 μseconds (90°); contact time, 1 millisecond; recycle time, 5 seconds. Free induction decays were acquired and zero-filled to 8K prior to Fourier Transformation. Up to 10,000 scans were collected for sufficient signal/noise. The Hartman–Hahn match was set using hexamethylbenzene, which was also used as a secondary external reference that gives the methyl peak, $\delta_C = 17.3$ ppm on the tetramethylsilane scale (^{13}C TMS = 0 ppm).

Thermogravimetric Analysis (TGA)

Chitosan adhesive films without IG dye were analyzed using a Perkin Elmer Pyris 1 Thermogravimetric Analyser to evaluate the water content and degradation temperature of the films in air (weight 10–15 mg). The temperature was increased from 20 to 600°C at a rate of 40°C/minute. The mass of five samples was continuously recorded as a function of temperature and the first derivative calculated to assess the adhesive degradation (derivative minimum peak) and water content (derivative = 0).

Contact Angle

The static contact angle of chitosan adhesives was measured by the sessile drop method using the RHI system (model 100-00-230, Landing, NJ). Six readings from different parts of the film surface were averaged to give the mean contact angle.

Adhesive Attenuation

A UV-Visible spectrophotometer was used to measure the laser attenuation at 808 nm within the films and to observe the attenuation characteristics of the adhesive due to the presence of IG. The wavelength of 808 nm corresponds to the absorption peak of IG and to the laser radiation used for laser tissue repair [2]. Adhesive films were fixed inside a plastic cuvette and placed in the light beam. The attenuation length (1/e attenuation) was calculated by assuming the validity of Beer's law: $I = I_0 e^{-A}$, where I_0 is the incident beam intensity and A is the film attenuation. The attenuation measurements were performed with baseline subtraction.

Laser Tissue Repair (LTR)

Tissue repair was investigated in this study using a GaAlAs diode laser (Qphotonics, L.L.C., VA), coupled with a multimode optical fiber through an FC connector. The fiberoptic cable was inserted in a hand-held probe to provide easy and precise beam delivery by the operator (fiber core diameter 200 μm, numerical aperture 0.22). The laser emitted at 808 nm, with an output power of 0.12 ± 0.01 W and beam spot size on the adhesive of approximately 1 mm, corresponding to an irradiance of $\sim$15 W/cm^2. Because the laser is not eye safe (Class IV), safety goggles were worn by all staff in the operating theatre.

The diode laser was used to irradiate the chitosan-based adhesive strips to repair rectangular sections of sheep small intestine ($\sim 2 \times 0.5$ cm) under an operative microscope ($\times 20$). Fresh intestinal tissue was harvested from sheep immediately after euthanasia and stored at -80°C. Prior to use, tissue was immersed in deionized water for 15 minutes to defrost and hydrate at room temperature. The serosa layer of intestine consists of connective tissue that is rich in collagen and therefore suitable for testing the tensile strength of laser adhesive repairs. Intestine is abundant in the sheep body and a single animal can provide enough tissue for several trials.

Intestine sections (2 cm) were bisected by a full thickness incision with a #10 blade. The intestine was kept moist using deionized water; excess water was absorbed with sterile gauze or cotton tips prior to tissue repair. The incision stumps were approximated end-to-end and a chitosan strip was positioned across the incision on the serosa layer with microforceps ensuring full contact with the intestine. Thereupon, the surgeon irradiated the adhesive by moving continuously the beam across its surface at a speed of $\sim$1 mm/second and without charring or ablating the adhesive (Fig. 2). Moderate tissue shrinkage under the adhesive was observed during laser irradiation. All tissue repairs were performed using fixed laser power and solder surface area (Table 1). Control experiments for tissue repair were carried out as described above, using chitosan strips without IG and without the use of laser light.

Tensiometer Measures

The intestine was tested 10 minutes after tissue repair using a calibrated tensiometer (Instron Mini 55, Canton, MA) to assess the tensile strength of the repaired wound. Tissue was maintained in wet gauze after being repaired to mimic in vivo conditions and avoid sample desiccation. A specimen was clamped to the tensiometer using pneumatic grips, separating at a rate of 22 mm/minute until the adhesive failed. The maximum load under which the adhesive failed was recorded by Merlin IX software.

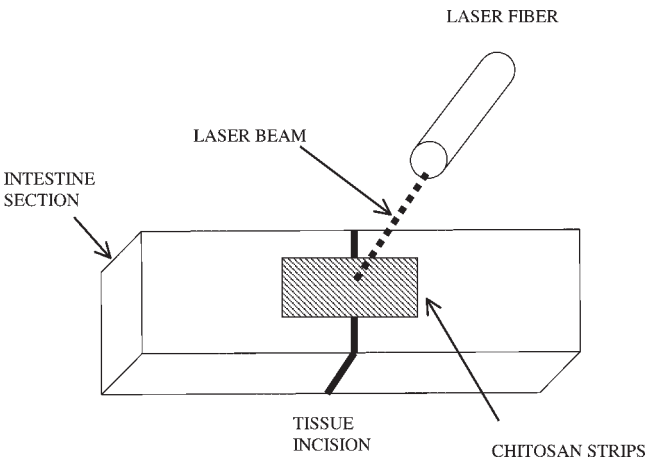

Fig. 2. Schematic top-view of laser tissue repairing. A strip of chitosan adhesive is applied across the incision then subsequently irradiated using a laser.

Rectangular strips of chitosan adhesive without IG dye and without laser activation were also tested alone by the tensiometer to measure their Young's modulus (E). The strips were wet with water and fixed to the grips, which moved apart until the repair failed. The software generated a strain-stress plot and calculated E in the strain region between 10% and 20%, assuming the strip thickness remained constant throughout elongation.

Temperature Measures

The temperature of LTR was measured with an insulated K-type thermocouple (diameter = 0.25 mm, response time = 0.1 second) positioned between the intestine and adhesive as illustrated in Figure 3. The thermocouple was connected to a signal-conditioning unit (SCXI-1121) with 4 Hz low pass analogue filter. Data were sampled at 10 Hz with a 12-bit data acquisition board (PCI-6024E) controlled by LabView® (National Instruments, Austin, TX) The strips were irradiated, as described previously, by moving continuously the beam across the adhesive surface; temperature data were recorded for 20 seconds while the beam was directed on the thermocouple or in its proximity. After LTR, the adhesive was detached using microforceps to ensure that tissue adhesion occurred.

Cytotoxic Assay

A cell growth inhibition assay was used to assess the cytotoxic potential of the chitosan adhesive films. Inhibition of cell growth in contact with extracts from these samples was compared with untreated medium and positive controls containing 7.5% ethanol. Murine L929 cells (Earle's L Cells-NCTC Clone 929) were established at $\sim 10^5$ cells per 35 mm diameter petri dishes. Cells were incubated at 37°C for 24 hours in a 5% CO_2 humidified atmosphere using Earle's minimum essential medium (EMEM) supplemented with 10% fetal bovine serum. After 24 hours, a sub-confluent cell monolayer was established and the medium was aspirated from the petri dishes. The medium was replaced with either a medium extract of the chitosan adhesives or with the controls.

All solder samples were γ-radiated in sealed sterifilm® at a level of $\sim$2.4 kGy to ensure sterile conditions (0.1 kGy/hour for 24 hours). Chitosan films with thickness of ~ 45 μm and surface area of ~ 18 cm^2 were extracted in 3 ml medium (EMEM) in glass vials for 24 hours at 37°C. The extract was removed and placed directly on the cell monolayer for 48 hours. During this time any cytotoxic components emanating from the test materials would have disrupted the growth of cells in the culture dish. At the end of the test period, cells were harvested, their numbers assessed through flow cytometry and compared with untreated cultures (null samples). Assessment via flow cytometry was facilitated by the addition of propidium iodide (10 μg/ml), which stains non-viable cells with a disrupted membrane. Cells were harvested into a known volume and a known number of ~ 10 μm diameter polystyrene beads was added to the cell suspension. The number of cells in suspension

TABLE 1. Laser Parameters and Adhesive Characteristics (Mean ± SD) Are Given for the Repairing of Rat Intestine

	Thickness (μm)	Area (mm^2)	Power (W)	Time (seconds)	Maximum load (N)	Tensile strength (kPa)
Chitosan + laser ($N = 30$)	20 ± 5	34 ± 4	0.12 ± 0.01	147 ± 7	0.50 ± 0.15	14.7 ± 4.7
Chitosan ($N = 30$)	20 ± 5	34 ± 4	NA	NA	0.08 ± 0.04	2.4 ± 1.2

N, number of laser-adhesive repairs; thickness, adhesive thickness; area, averaged adhesive surface area in contact to the intestine during laser repair; power, laser power during tissue repair; time, laser irradiation time; max load, maximum load in Newtons under which the tissue repairs failed; tensile strength, maximum load divided by the surface area of the chitosan adhesive.

was back calculated by comparing the ratio of cells to beads acquired by flow cytometry. Viability staining, forward scatter and side scatter evaluation by flow cytometry provided a more sensitive indication of material toxicity than inhibition alone.

Statistical comparison of means was made using ANOVA one-way and Bonferroni's multiple comparison tests at 0.05 level of significance; Excel 2000 generated the histograms.

RESULTS

^{13}C-NMR

The solid-state ^{13}C-NMR spectra of commercially available chitosan, and the chitosan adhesive are displayed in Figure 4a,b respectively. No significant chemical change occurred during the preparation of chitosan adhesive. In both spectra there are the peaks expected for the glucosamine moiety at ~104(C1), 77(C3–5), 57(C2, C6) ppm. In the commercial chitosan sample the peaks for the residual acetate group from the unhydrolysed chitin at ~174(C=O) and 24(CH_3) ppm could be readily observed, while in that for the chitosan adhesive, the acetate peaks are augmented by the acetic acid used in the preparation of the adhesive [21]. The peaks are relatively broad reflecting the amorphous nature of these materials.

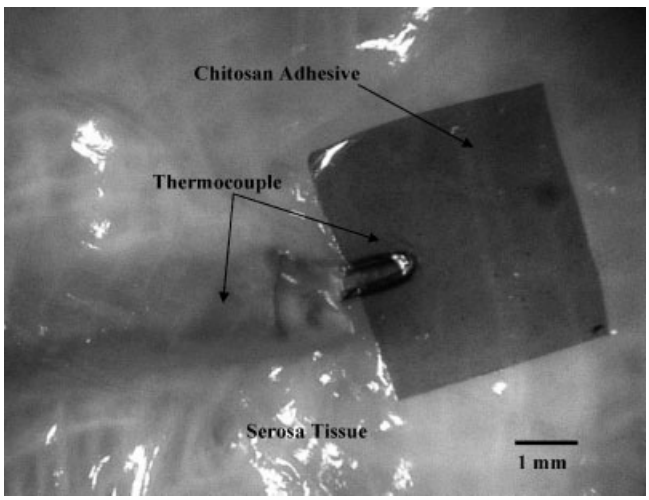

Fig. 3. Photograph showing a strip of chitosan adhesive bonded to the serosa layer of intestine. A thermocouple was placed between tissue and adhesive to record the temperature during LTR.

TGA and Contact Angle

The TGA analysis showed an initial sample weight loss of 13.2% ± 0.4% (mean ± SD, $n = 5$) that remained constant up to 211 ± 13°C (Fig. 5). It is most likely that during this phase water evaporated. The adhesive degraded and its weight diminished to 37.4% ± 1.5% at 317 ± 1°C, the temperature of maximum rate of weight loss (derivative minimum peak).

The contact angle of the adhesive was 47 ± 4° ($n = 6$), consistent with a moderately hydrophilic nature.

Temperature Measures

The temperature for LTR with chitosan adhesive was 57 ± 5°C (Fig. 6). The laser output raised sporadically the temperature to a maximum level of ~65°C and this always resulted in charring of the adhesive. Moderate tissue shrinkage under the adhesive was observed whenever the thermocouple measured temperatures above 60°C. The irregular profile of the temperature plots in Figure 6 is a reflection of the free hand use of the laser and is typical of surgical procedures.

Tensiometer Measures

The laser-irradiated strips of chitosan fully bonded to tissue and withstood a maximum load of 0.50 ± 0.15 N (tensile strength = 14.7 ± 4.7 kPa, mean ± SD, $n = 30$). Strips without the laser irradiation step resulted in a significantly lower bonding strength of 0.08 ± 0.04 N (tensile strength = 2.4 ± 1.2 kPa, $n = 30$, $P \ll 0.05$, unpaired *t*-test). The strips failed at the tissue interface, without breaking, in both types of repair procedures (Fig. 7, Table 1).

Young's modulus for wet strips of adhesive, prior to laser radiation, was 6.81 ± 1.26 MPa ($n = 15$). The adhesive not only showed cohesive strength but also flexibility as it could be flexed to ~160° without suffering macroscopic damage. The tensile test results are summarized in Figure 8.

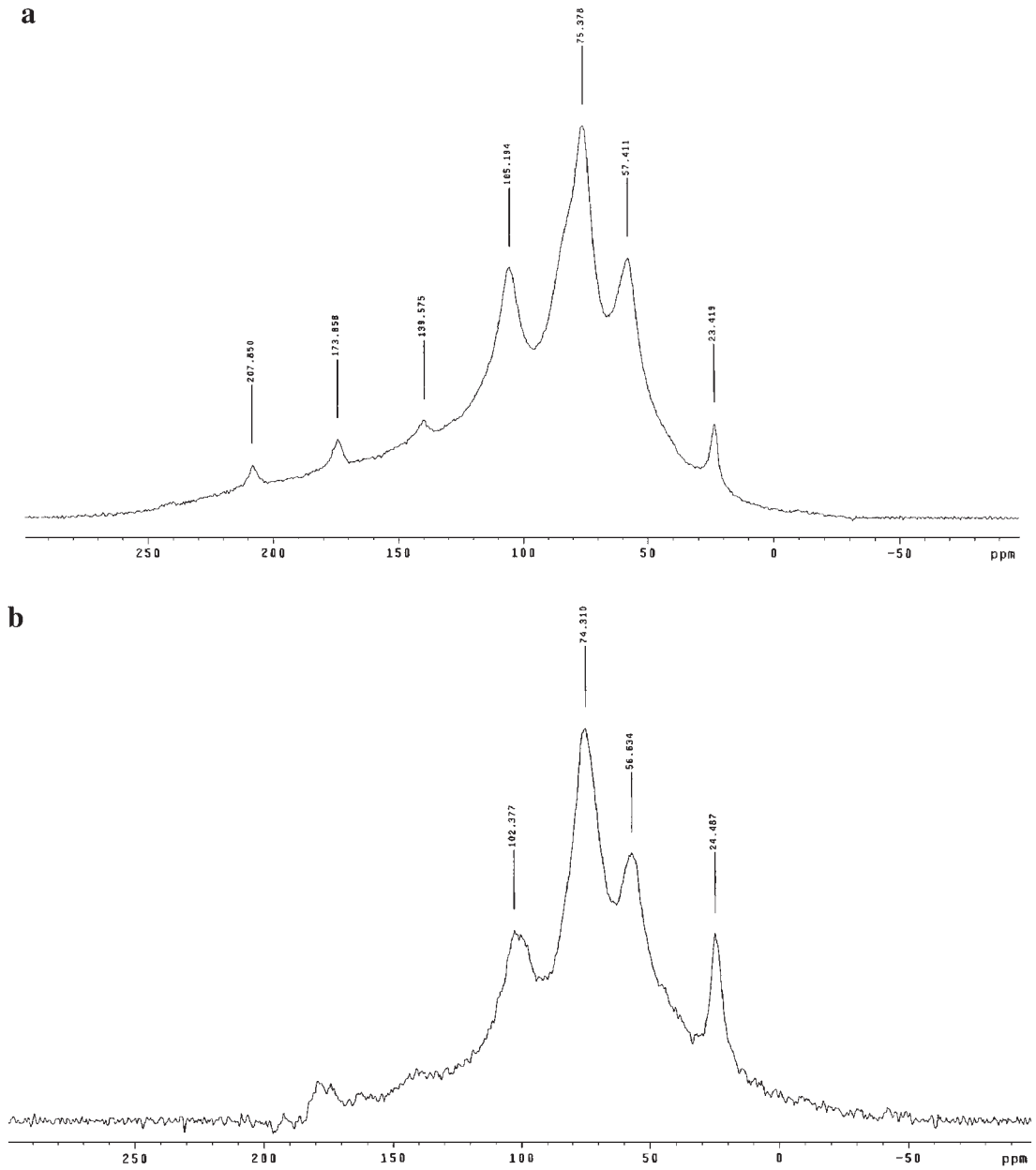

Fig. 4. ^{13}C-NMR spectra of chitosan shells (**a**) and adhesive (**b**). The glucosamine moiety at ~104(C1), 77(C3–5), 57(C2, C6) ppm, are present in chitosan shells and adhesive. The residual acetate group from the unhydrolysed chitin, at ~174(C=O) and 24(CH_3) ppm are augmented in the adhesive spectrum by acetic acid. No significant chemical changes occurred during the preparation of the chitosan adhesive.

Adhesive Attenuation

The attenuation length of the chitosan adhesive with and without IG at 808 nm were respectively 5 ± 1 μm and 228 ± 72 μm ($n = 3$). Assuming insignificant scattering and reflection, we may ascribe to IG the efficient absorption of the laser energy inside the chitosan adhesive, which prevented IR radiation to directly affect the thermocouple and alter the temperature measures. In contrast, chitosan adhesive without IG was virtually transparent to the laser (Fig. 9, Table 2).

Cytotoxicity Tests

The chitosan adhesive appeared to induce negligible cytotoxicity (Fig. 10). One-way variance analysis indicated a significant difference between the controls and experimental groups ($P < 0.0001$). In particular, there was no statistical difference between the cell number of the null

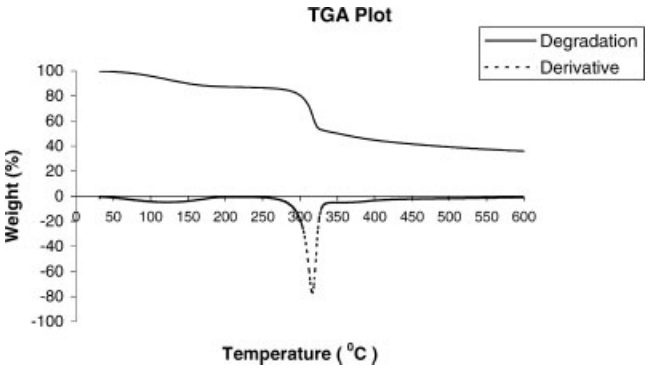

Fig. 5. The weight loss of chitosan adhesive is given as a function of temperature. Water evaporated up to 211°C, reducing the adhesive weight of 13% (first derivate = 0). The adhesive burnt at ~317°C, where the weight loss rate achieved its maximum (minimum peak of the first derivative).

($n = 3$), blank ($n = 6$), and chitosan extracted samples ($n = 9$, cell number $> 280 \times 10^3$, $P > 0.05$, Bonferroni's post-test). The growth of cells treated with ethanol ($n = 3$) was significantly inhibited when compared to the growth of the chitosan extracted samples and negative controls (cell number $< 55 \times 10^3$, $P < 0.001$, Bonferroni's post-test). Viability of the cells cultured in the chitosan extract, null and blank were greater than 95%, while cells cultured in the 7.5% ethanol control had a viability of 53%. Forward and side scatter provided a qualitative evaluation of cell health; cells cultured in chitosan extract appeared equivalent to cells harvested from the blank or null. The addition of 7.5% ethanol to culture media resulted in a qualitative changes to the cell shape, which was easily observed in their forward and side scatter. This detailed evaluation allowed for detection of toxic properties at doses lower than what would be statistically detectable in growth inhibition and confirmed the non cytotoxic properties of the chitosan adhesive.

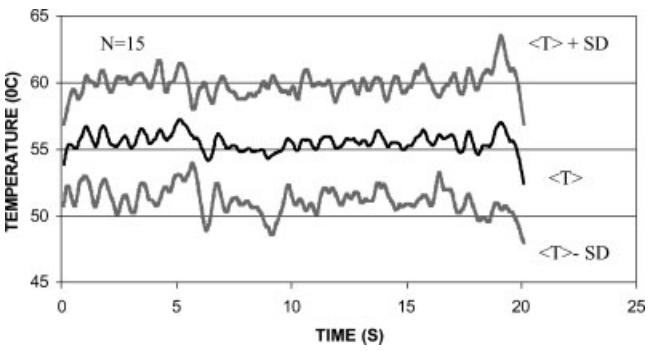

Fig. 6. Graph illustrating the temperature of the thermocouple, under the chitosan adhesive at tissue interface, as a function of time. The mean temperature ± standard deviation ($n = 15$) is also provided to indicate the temperature range during LTR.

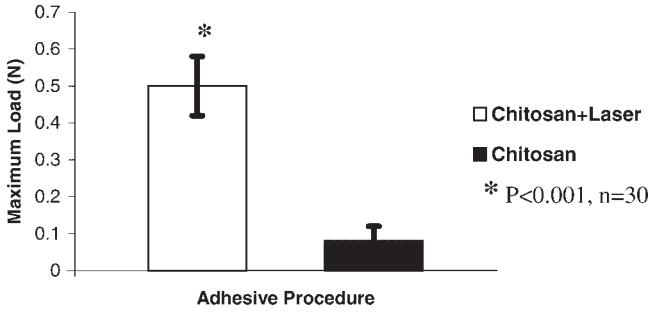

Fig. 7. Histogram of acute tensile strength of chitosan adhesive with and without the aid of laser radiation (mean ± SD).

DISCUSSION

In this communication, we report on the development of a novel light-activated adhesive that is insoluble in water and has improved mechanical properties compared with existing solders. The chitosan adhesive bonded to sheep intestine with a high tensile strength (~14.7 kPa, maximum load ~0.50 N) and also demonstrated a high E modulus of ~6.8 MPa, which resulted in all the adhesive strips investigated detaching from the tissue without breaking. When compared to conventional albumin-based solders, the chitosan adhesive strips proved to withstand a higher maximum load than that of albumin strips with similar dimensions [13]. The laser-activated adhesive was also stronger than the soluble chitosan gel, which was modified with UV crosslinkers (tensile strength ~3.1 kPa) [20].

Chitosan adhesive strips demonstrated an initial adhesion to tissue prior to laser irradiation (tensile strength ~2.4 kPa), in agreement with previous reports [22].

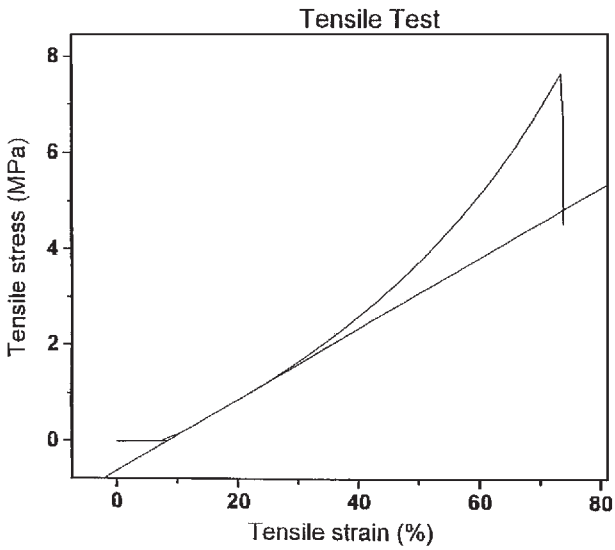

Fig. 8. Graph illustrating the stress and strain relationship for wet chitosan adhesive. The E modulus (~6.8 MPa) was calculated in the strain region between 10% and 20%, where the adhesive shows its elastic behavior.

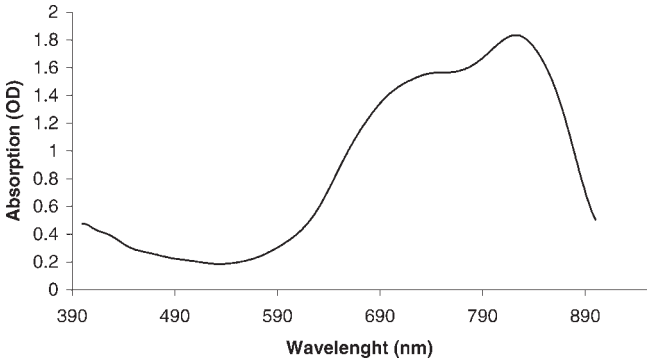

Fig. 9. Typical attenuation spectrum of chitosan adhesive in the visible-NIR region. A strong attenuation peak is localized at 808 nm, corresponding to the well-known absorption wavelength of indocyanin green (IG) dye.

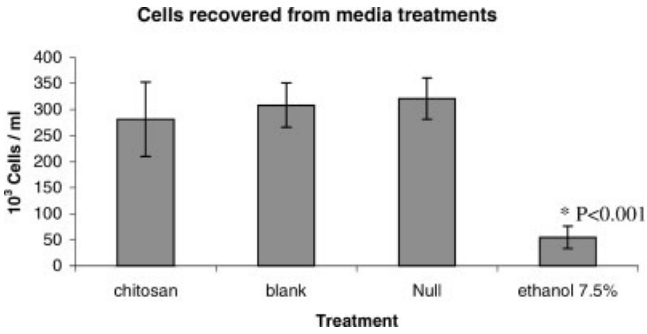

Fig. 10. Histogram illustrating the number of cells recovered as a function of media treatment (mean ± standard deviation). The chitosan adhesive extracts were not cytotoxic to fibroblasts when compared to the null and blank. Solutions 7.5% ethanol significantly inhibited cell growth (positive controls). Ethanol, samples of cells exposed to media with ethanol at 7.5% concentrations (v/v). Null, sample of cells exposed to fresh media. Blank, sample of cells exposed to media, which was incubated for 24 hours in 5% CO_2 air at 37°C. Chitosan adhesive, samples of cells exposed to media, which was incubated with chitosan adhesive for 24 hours in 5% CO_2 air at 37°C.

Such adhesiveness was greatly enhanced by the laser as the IG dye converted photons into heat that supposedly diffused to the tissue interface, enhancing the bonding between chitosan and tissue. The mechanism responsible for this photo-adhesiveness is not clear yet, although we may hypothesize that polyanionic-polycationic interactions and hydrogen bonding occurred between chitosan and collagen, as previously reported [18,19]. Specific studies are necessary to elucidate the type of bonding responsible for the adhesiveness of laser activated chitosan films.

No evident damage such as vacuoles or carbonization was observed on the serosa beneath the adhesive, after laser irradiation. These preliminary microscopical observations were most likely due to the low levels of power and fluence, which raised the average temperature at the tissue interface from 57 to 62°C. It should be noted that the temperatures recorded by the thermocouple are an estimation of the real temperatures of the tissue interface during LTR. These measures were subjected to errors, mainly due to the thermocouple mass and the limited surface area of the adhesive probed by the thermocouple. The latter error was due to the small diameter of the thermocouple bed; this resulted in a significant temperature drop whenever the laser beam was not in the thermocouple proximity. The error due to the thermocouple mass was estimated to be ~2°C. The above considerations indicate that <T> + standard deviation (~62°C) should be the closest estimation of the true temperature at the tissue interface during LTR (Fig. 6). In addition, the moderate tissue shrinkage observed during LTR indicated that the tissue temperature might have ranged between 60 and 65°C [23]. Such temperatures appear to be significantly lower than the temperatures used for LTR with albumin solders. In these cases, the albumin needs to be denatured at 65–70°C to create a strong, insoluble bond to tissue [11,12,24]. In contrast, chitosan adhesives are stable up to ~200°C (Fig. 6) and do not denature, liquefy, or melt like protein solders. One may assume that only the tissue collagen has to denature at 60–65°C prior to bonding to chitosan and renaturing upon cooling to substantially increase the initial adhesiveness of chitosan films [25–27].

TABLE 2. Attenuation Data of the Adhesive at a Wavelength of 808; the Mean Value ± the Standard Deviation Are Given

	λ (nm)	Thickness (μm)	Attenuation length (μm)
Chitosan + IG ($N = 3$)	808	30 ± 10	5 ± 1
Chitosan ($N = 3$)	808	30 ± 10	228 ± 72

N, number of adhesive samples analyzed; attenuation length, 1/e attenuation of the chitosan adhesive, as calculated from Beer's law; thickness, thickness of chitosan adhesives.

It is very important that tissue glues, solders, and adhesives are not altered or degraded by aqueous solutions such as physiological fluids, which are often used to maintain the moisture of exposed tissues at operated sites. It was noticed during our experiments that the chitosan adhesives swelled, curled, and dissolved in water, if not dried thoroughly. Particular attention was therefore necessary to dry the films until they became insoluble.

In contrast to albumin solders, chitosan adhesives not only have the notable property of being insoluble but also exhibit important mechanical properties such as high E modulus and flexibility. Adhesives with ~20 μm thickness could sustain a stress of ~14.7 kPa without breaking, had an E modulus of 6.8 MPa and could be curved or deformed over 160°, returning to their initial shape with no sign of macroscopic damage. This flexibility of the chitosan adhesive allowed the surgeon to manipulate tissue without fear of it breaking or tearing. The adhesive did not fold or breakdown when manipulated with forceps and appeared

to be well suited for tissue repair. The application of the adhesive chitosan films on tissue prior to laser activation is also facilitate by its hydrophilic and adhesive properties.

Unlike fibrinogen and albumin based solders which are derived from blood-based proteins, the chitosan adhesive is based on a polysaccharide and consequently there are no risks of viral infections associated to this novel adhesive. Furthermore, Chitosan is widely accepted as a non-toxic and biocompatible polysaccharide. Among other applications, chitosan is employed to develop skin grafts, tissue scaffolds and dietary products [28–32]. Also of consideration in tissue repair is the remarkable antimicrobial properties of chitosan, which reduces potential infection [16,33].

According to ^{13}C-NMR, the laser-activated adhesive has the same chemical composition of chitosan shells derived from marine crustacean and therefore should retain the above mentioned properties of biocompatibility and non toxicity (Fig. 4). The results of cytotoxicity test support this suggestion, with media extracted from the adhesive showed negligible toxicity to fibroblasts [34].

Chitosan adhesives may degrade in the body and also act as a delivery system at the repair site, with the potential of incorporating therapeutic drugs such as growth factors, antibiotics, or genes to guide and enhance the wound healing process [35,36].

It has been shown that in vitro and in vivo degradation of chitosan films occurred less rapidly as the film deacetylation became higher [37]. Chitin films were implanted in the back of rats and degraded ~25% in 2 weeks, while chitosan films (85% deacetylated) degraded 20% in 12 weeks. Furthermore, lysozyme degradation of chitosan has been reported [37,38]. For example, 10% of chitosan films (85% deacetylated) degraded in 48 hours if incubated in buffered aqueous solution (pH ~7) with lysozyme (4 mg/ml) at 37°C [37].

Chitosan adhesives may be manufactured in a broad spectrum of shapes and dimensions to suit the organ or tissue characteristics where they are applied. Further studies are currently in progress to assess the efficacy and safety of chitosan adhesives in animal models.

ACKNOWLEDGMENTS

The authors thank Daniel Di Giusto, Dr. Garry King, Dr. Zhang, Dr. Lamb, Dr. Phil Preston, John Rawlinson, and Damia Mawad for their kind help.

REFERENCES

1. Poppas DP, Schlossberg SM, Richmond IL, Gilbert DA, Devine CJ, Jr. Laser welding in urethral surgery: Improved results with a protein solder. J Urol 1988;139(2):415–417.
2. Oz MC, Johnson JP, Parangi S, Chuck RS, Marboe CC, Bass LS, Nowygrod R, Treat MR. Tissue soldering by use of indocyanine green dye-enhanced fibrinogen with the near infrared diode laser. J Vasc Surg 1990;11(5):718–725.
3. Forman SK, Oz MC, Lontz JF, Treat MR, Forman TA, Kiernan HA. Laser-assisted fibrin clot soldering of human menisci. Clin Orthop 1995;310:37–41.
4. Small W IV, Heredia NJ, Maitland DJ, Da Silva LB, Matthews DL. Dye-enhanced protein solders and patches in laser-assisted tissue welding. J Clin Laser Med Surg 1997; 15(5):205–208.
5. Mueller MP, Kopchok GE, Tabbara MR, Cavaye DM, White RA. Argon laser-welded bovine heterograft anastomoses. J Clin Laser Med Surg 1993;11(1):1–5.
6. Hino M, Ishiko O, Honda KI, Yamane T, Ohta K, Takubo T, Tatsumi N. Transmission of symptomatic parvovirus B19 infection by fibrin sealant used during surgery. Br J Haematol 2000;108(1):194–195.
7. Kasper CK. Concentrate safety and efficacy. Haemophilia 2002;8(3):161–165.
8. Kirsch AJ, Cooper CS, Gatti J, Scherz HC, Canning DA, Zderic SA, Snyder HM III. Laser tissue soldering for hypospadias repair: Results of a controlled prospective clinical trial. J Urol 2001;165(2):574–577.
9. Maitz PKM, Trickett RI, Dekker P, Tos P, Dawes JM, Piper JA, Lanzetta M, Owen ER. Sutureless microvascular anastomoses by a biodegradable laser-activated solid protein solder. Plast Reconstr Surg 1999;104(6):1726–1731.
10. Lauto A, Dawes J, Piper J, Owen R. Laser nerve repair by solid protein band technique. II: Assessment of long term regeneration. Microsurgery 1998;18:60–64.
11. Fung LC, Mingin GC, Massicotte M, Felsen D, Poppas DP. Effects of temperature on tissue thermal injury and wound strength after photothermal wound closure. Lasers Surg Med 1999;25(4):285–290.
12. Simhon D, Ravid A, Halpern M, Cilesiz I, Brosh T, Kariv N, Leviav A, Katzir A. Laser soldering of rat skin, using fiberoptic temperature controlled system. Lasers Surg Med 2001;29(3):265–273.
13. Lauto A, Foster J, Ferris L, Avolio A, Zwaneveld Nick, Poole-Warren L. Albumin–genipin solder for laser tissue-welding. Lasers Surg Med 2004;35(2):140–145.
14. Lauto A, Ohebshalom M, Esposito M, Mingin J, Li PS, Felsen D, Goldstein M, Poppas DP. Self-expandable chitosan stent: Design and preparation. Biomaterials 2001;22:1869–1874.
15. Shigemasa Y, Shibazaki K, Minami S, Matsuhashi A, Tanioka S, Shigemasa Y. Evaluation of chitin and chitosan for biomaterials. Biotech Genet engineer Rev 1996;13:383–420.
16. Muzzarelli R, Tarsi R, Filippini O, Giovanetti E, Biagini G, Varaldo PE. Antimicrobial properties of *N*-carboxylbutyl chitosan. Antimicro Ag Chemotherap 1990;34:2019–2023.
17. Rao SB, Shorma CP. Use of chitosan as a biomaterial: Studies on its safety and homeostatic potential. J Biomed Mater Res 1997;34:21–28.
18. Taravel MN, Domard A. Relation between the physicochemical characteristics of collagen and its interactions with chitosan: I. Biomaterials 1993;14(12):930–938.
19. Taravel MN, Domard A. Collagen and its interaction with chitosan. II. Influence of the physicochemical characteristics of collagen. Biomaterials 1995;16(11):865–871.
20. Ono K, Saito Y, Yura H, Ishikawa K, Kurita A, Akaike T, Ishihara M. Photocrosslinkable chitosan as a biological adhesive. J Biomed Mater Res 2000;49:289–295.
21. Heux L, Brugnerotto J, Desbrieres J, Versali M-F, Rinaudo M. Solid state NMR for determination of degree of acetylation chitin and chitosans. Biomolecules 2000;1:746–751.
22. Needleman IG, Smales FC, Martin GP. An investigation of bioadhesion for periodontal and oral mucosal drug delivery. J Clin Periodontol 1997;24(6):394–400.
23. Naseef GS III, Foster TE, Trauner K, Solhpour S, Anderson RR, Zarins B. The thermal properties of bovine joint capsule. The basic science of laser- and radiofrequency-induced capsular shrinkage. Am J Sports Med 1997;25(5): 670–674.
24. Simhon D, Brosh T, Halpern M, Ravid A, Vasilyev T, Kariv N, Katzir A, Nevo Z. Closure of skin incisions in rabbits by laser soldering: I: Wound healing pattern. Lasers Surg Med 2004; 35(1):1–11.
25. Moran K, Anderson P, Hutcheson J, Flock S. Thermally induced shrinkage of joint capsule. Clin Orthop 2000;381: 248–255.

26. McClain PE, Wiley ER. Differential scanning calorimeter studies of the thermal transitions of collagen. Implications on structure and stability. J Biol Chem 1972;247(3):692–697.
27. Wall MS, Deng XH, Torzilli PA, Doty SB, O'Brien SJ, Warren RF. Thermal modification of collagen. J Shoulder Elbow Surg 1999;8(4):339–344.
28. Azad AK, Sermsintham N, Chandrkrachang S, Stevens WF. Chitosan membrane as a wound-healing dressing: Characterization and clinical application. J Biomed Mater Res 2004; 6B(2):216–222.
29. Stone CA, Wright H, Clarke T, Powell R, Devaraj VS. Healing at skin graft donor sites dressed with chitosan. Br J Plast Surg 2000;53(7):601–606.
30. Hsu SH, Whu SW, Hsieh SC, Tsai CL, Chen DC, Tan TS. Evaluation of chitosan–alginate–hyaluronate complexes modified by an RGD-containing protein as tissue-engineering scaffolds for cartilage regeneration. Artif Organ 2004;28(8): 693–703.
31. Ylitalo R, Lehtinen S, Wuolijoki E, Ylitalo P, Lehtimaki T. Cholesterol-lowering properties and safety of chitosan. Arzneimittelforschung 2002;52(1):1–7.
32. Gades MD, Stern JS. Chitosan supplementation and fecal fat excretion in men. Obes Res 2003;11(5):683–688.
33. Rabea EI, Badawy ME, Stevens CV, Smagghe G, Steurbaut W. Chitosan as antimicrobial agent: Applications and mode of action. Biomacromolecules 2003;4(6):1457–1465.
34. Guggi D, Langoth N, Hoffer MH, Wirth M, Bernkop-Schnurch A. Comparative evaluation of cytotoxicity of a glucosamine-TBA conjugate and a chitosan-TBA conjugate. Int J Pharm 2004;278(2):353–360.
35. Chourasia MK, Jain SK. Design and development of multiparticulate system for targeted drug delivery to colon. Drug Deliv 2004;11(3):201–207.
36. Bozkir A, Saka OM. Chitosan nanoparticles for plasmid DNA delivery: Effect of chitosan molecular structure on formulation and release characteristics. Drug Deliv 2004; 11(2):107–112.
37. Tomihata K, AndIkada Y. In vitro and in vivo degradation of films of chitin and its deacetylated derivates. Biomaterials 1997;18:567–575.
38. Lee KY, Ha WS, Park WH. Blood compatibility and biodegradability of partially *N*-acylated chitosan derivates. Biomaterials 1995;16:1211–1216.